Relaxation of the magnetization of Mn_{12} acetate

J. A. A. J. Perenboom
Research Institute for Materials and High Field Magnet Laboratory, University of Nijmegen, NL-6525 ED Nijmegen, The Netherlands

J. S. Brooks and S. Hill
Department of Physics and National High Magnetic Field Laboratory, Florida State University, Tallahassee, Florida 32310

T. Hathaway and N. S. Dalal
Department of Chemistry and National High Magnetic Field Laboratory, Florida State University, Tallahassee, Florida 32310

(Received 4 August 1997)

The magnetization of a Mn_{12}-acetate single crystal was measured with a cantilever magnetometer to temperatures below 60 mK. Contrary to expectations we did not observe steps in the hysteretic magnetization with indices higher than 11. The data suggest a significant degree of higher-order anisotropy. The fourth-order term appears to be about $-3\times10^{-4}k_B$. Both hysteresis in magnetization at different ramping rates of the field, and relaxation at different fixed values of the magnetic field were studied. The relaxation is found to be logarithmic below 1 K, and not single exponential. We contend that the process of magnetization reversal is initiated by tunneling across the anisotropy barrier from a weak population in excited levels from which they can easily tunnel across the barrier, and that the consequent emission and reabsorption of phonons helps to promote a significant fraction of the spins to these excited levels.
[S0163-1829(98)02525-9]

INTRODUCTION

The Mn_{12}-acetate complex first synthesized by Lis,[1] $[Mn_{12}O_{12}(CH_3COO)_{16}(H_2O)_4]\cdot 2CH_3COOH\cdot 4H_2O$, has attracted strong interest because it may be a system exhibiting macroscopic quantum tunneling of magnetic moment (QTM). The quantum steps in the hysteresis loop observed at temperatures below about 3 K in oriented powder samples[2–4] and somewhat later in a single crystal[5] are a dramatic demonstration of the resonant nature of the magnetization reversal. These steps corroborate early indications of quantum tunneling believed to be found in the saturation of the relaxation time at low temperatures.[6] Very recently indications for QTM were also found in a Fe_8 cluster.[7]

The core of the compound consists of a tetrahedron of four Mn(IV) ions each in their $S=\frac{3}{2}$ state, surrounded by eight Mn(III) ions each with $S=2$. The Mn ions are linked by triply bridging oxo-O atoms and by carboxylate bridges from acetate anions.[1] Superexchange along the oxygen bridges connecting the Mn ions leads to a high spin ground state where the spins of the Mn(IV) and Mn(III) ions are coupled parallel to $S=6$ and $S=16$, respectively. On the other hand, the spins of the outer shell are directed antiparallel to the spins of the inner ions to lead to a total spin $S=10$.[8,9] Estimates of the strength of the spin-spin interactions[8] indicate that the strongest contribution will be between ions on the inner tetrahedron and ions on the outer shell with $J\approx -215k_B$. Therefore at low temperatures the Mn_{12} cluster can be treated effectively as a single $S=10$ system. The clusters crystallize into a tetragonal lattice, the angular momentum is completely quenched and the Jahn-Teller distortion [which is known to be significant for the Mn(III) positions] combines to provide a strong axial anisotropy. High field magnetization and electron paramagnetic resonance (EPR) have indicated that the ground state is $m=\pm 10$, with the spin preferentially aligned along the c axis.[9] At low temperatures (below 10 K) there is no appreciable population left in the excited levels, and if a magnetic field is applied, and the $m=+10,-10$ degeneracy is removed, the clusters will become completely polarized. If the field is then reduced to zero (or inverted), the magnetization has to decay (or reverse to the opposite polarization), and ac-susceptibility measurements have suggested that the decay is single exponential and thermally activated,[10,11] $\tau=\tau_0\exp(K/k_BT)$, with K ranging from $64k_B$ to $61k_B$ and $\tau_0=2.6-2.1\times10^{-7}$ s. This relaxation is unusually slow. Below 3 K the relaxation time starts to exceed the time of measurement, and below this so-called ''blocking temperature,'' the magnetization becomes hysteretic. It was later found[6] that, at low temperatures, the relaxation time does not continue to grow exponentially but instead saturates at values of 10^7-10^8 s, i.e., many months. This was taken as evidence that the mechanism of relaxation is quantum tunneling of magnetization.

Despite these extensive studies, several basic issues remain unclear. First, how many steps can be detected in the hysteresis loop measurements? Second, how precisely does the relaxation rate obey a single exponential behavior? Third, how accurately does the relaxation rate become temperature independent at low temperatures? This is quite important because it has been cited as major evidence for the relaxation process being quantum tunneling. The present investigation attempts to provide a more clear answer to all of these questions. In contrast to earlier studies we have used the cantilever technique with its high sensitivity and rapid response time, enabling studies on high-quality single crystals.

The details of the experimental procedure, the cantilever technique, and sample growth are described in the following

section. This is followed by the sections on experimental results and their theoretical interpretation, and by a summary of the major results.

EXPERIMENT

We have used a cantilever magnetometer[12] to study the magnetization of Mn_{12}-acetate single crystals, and the slow relaxation of the magnetic moment, in the temperature range from 3 K down to 50 mK. The cantilever technique is distinguished by its very high sensitivity, especially for axially oriented magnetic moments as in the case of the Mn_{12} clusters with their high c-axis anisotropy energy. In such a case it can be applied in the torque mode, and the torque trying to align the magnetic moment along (when $\mathbf{m}\|\mathbf{B}$) or away from (when $-\mathbf{m}\|\mathbf{B}$) the direction of the applied magnetic field will result in a small, capacitively detected deflection of the thin silicon cantilever. Near zero field, however, the sensitivity vanishes, but for fields above 0.5 T we obtain a very satisfactory signal-to-noise ratio with single crystals as small as 20 μg. The data down to 450–500 mK were obtained using a ^{3}He cryostat in the resistive magnets at NHMFL, while for the millikelvin data a dilution refrigerator in a superconducting magnet was used.

The Mn_{12}-acetate complex was synthesized following the original procedure described by Lis[1] [reaction of $Mn(CH_3COO)_2$ with $KMnO_4$ in 60% CH_3COOH]. The single crystals were grown by the slow evaporation technique, and grew in the form of rectangular parallel-pipeds with the longest dimension as the c axis (which is also the direction of easy magnetization). The sample authenticity was confirmed by dc-magnetic-susceptibility data which showed excellent agreement with respect to the transition anomaly below 3 K as well as hysteresis and steps in the magnetization loop at temperatures below 3 K. The crystals utilized were approximately 0.015 mm^3 with 0.8 mm as the largest dimension.

THE MAGNETIZATION

Figure 1 shows some typical magnetization curves (normalized to the saturation value at higher fields) for temperatures from 2.8 down to 0.5 K. It is quite apparent that at the higher temperatures, steps are seen to occur at lower indexed transitions, while at the lowest temperature transitions at indices $N=7$, 8, 9, and 10 can be observed. The ramping rates were normally 0.0085 T/s.

It seems worthwhile here to discuss the general appearance of the capacitance data: Figs. 2(a) and 2(b) show the change of capacitance corresponding to the magnetization of the clusters. The general appearance of the capacitance change can be understood as follows: for much of the curve the magnetization of the Mn_{12} clusters is saturated to the full $M_s=\pm g\mu_B S/V_0$, where $V_0=3716$ Å^3 is the volume of the unit cell, so that $\mu_0 M_s \approx 0.06$ T. The magnetic moment $m=MV$ is first aligned along the magnetic field while the field is reduced from an initially high value (around 9 T in most of our measurements) and then antiparallel to the field as the direction of the applied magnetic field is reversed. We can expect a small misalignment (less than a degree is more than enough), and with $\mathbf{m}\|\mathbf{B}$ the sample will be drawn closer to

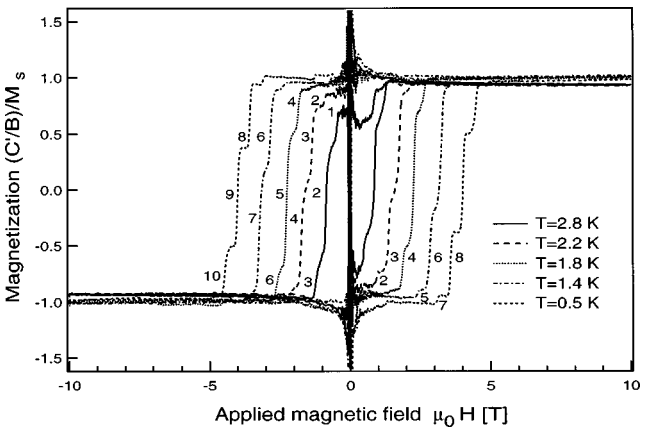

FIG. 1. Magnetization (normalized to the saturation magnetization M_s) for a Mn_{12}-acetate single crystal with the magnetic field aligned parallel to the easy axis, and for several different temperatures from 2.8 down to 0.5 K. The sample is first fully magnetized; rapid changes in magnetization occur at regular intervals after the field has been reversed, and we can distinguish steps with indices 1 through 10.

the direction of the field and the torque exerted by the field on the constant magnetic moment will decrease as the alignment improves so that the incremental effect on the capacitance gets smaller. On the other hand, when $-\mathbf{m}\|\mathbf{B}$, the moment will be rotated away from the direction of the field and the torque exerted by the field on the constant magnetic moment will instead increase and we see an increasingly strong response of the capacitance with deflection in the region between zero field and where the steps are first observed and the magnetization starts to reverse. Although the samples were small, the signals were strong for the cantilever magnetometer amounting to changes of the capacitance as much as 20%. The deflection of the capacitance plates is determined by balance of the torques due to the aligning magnetic field and to the elastic forces compensating the bending of the cantilever on the tip of which the sample is placed. In addition therefore, some nonlinearity in response may also result from the $1/d$ dependence of the capacitance on the

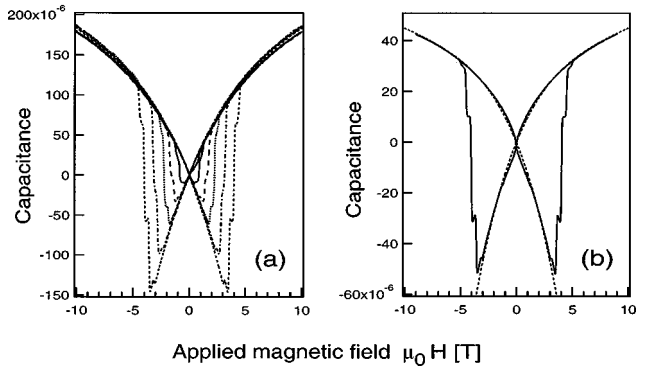

FIG. 2. Variation of the capacitance caused by the torque exerted by the magnetic field on the magnetic moment of the Mn_{12}-acetate single crystal; (a) corresponding to the magnetization curves of Fig. 1, measured in a resistive magnet, (b) for $T=443$ mK as measured in a superconductive magnet [the dashed lines represent $f(C)B$, the background used to calculate the instrumental correction factor].

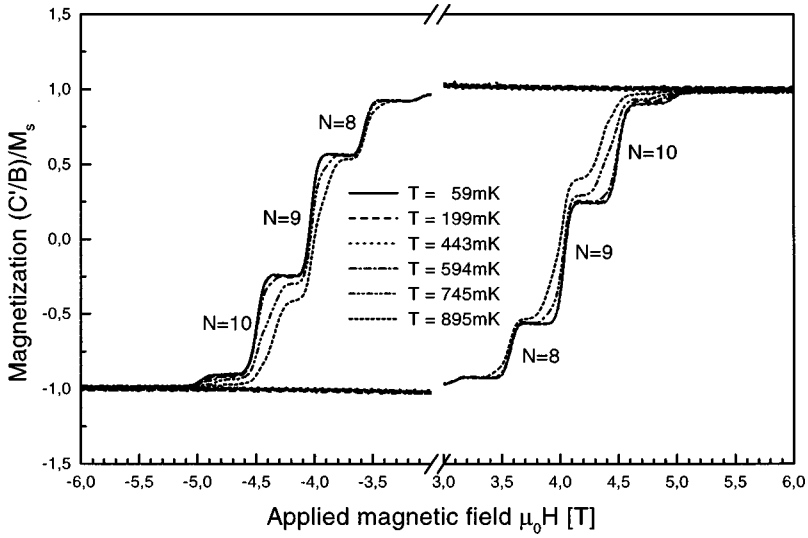

FIG. 3. Magnetization (normalized to the saturation magnetization) for a Mn_{12}-acetate single crystal for 59, 199, 443, 594, 745, and 895 mK showing steps at $N=7$, 8, 9, 10, and 11.

plate separation d (one may assume that they remain parallel to each other, as the change of angle of the capacitance plates is much less than a degree).

The magnetization is now found from the capacitance through division by B, and we take into account a capacitance-dependent instrumental factor $f(C)$ correcting the abovementioned nonlinear effects [it would have been more appropriate to define an instrumental function depending on the magnetic moment $f(m)$, but unlike the function $f(C)$ of the capacitance C, $f(m)$ would have suffered from a dependence on the sign of B]. The magnetic field axis was given by a signal proportional to the current fed to the magnet, and it is apparent in Fig. 2(b) that in the superconducting magnet at low fields there are features which we have attributed to deviations from a linear field-to-current relation for the superconducting magnet around $B=0$ and below 2 T. As a consequence the capacitance does not vary linearly with field in this range, resulting in a spurious signal C/B in the low-temperature measurements. As these effects are just outside the range of interest, we have chosen to ignore that region of magnetic fields.

The appearance of features in these magnetization curves is of course very much dependent on whether the time constant of the relaxation process corresponds to the measuring time. Thus far steps up to $N=6$ have been documented, but is is expected that many more should be detected at lower temperatures as the processes slow down. It has been mentioned,[3] for example, that indices up to $N=19$ should be observed with the temperature reduced to near 10 mK. It is our observation that this does not occur: the highest index step that we have observed is the $N=11$ transition, this step appears below 750 mK and accounts for the last 5% of magnetization reversal all the way down to 60 mK. Figure 3 shows a blow-up of some of the magnetization data obtained in the dilution refrigerator between 900 and 60 mK. It can be noted that the same steps are observed over the whole range of temperatures, and that within the accuracy of our measurement the slope dM/dB *at* the steps does not change much in this range of temperatures: as the temperature is lowered, there is a significant sharpening of the leading edge of the steps, and for temperatures below 500 mK all measured curves coincide. If we associate the change of magnetization in the leading edge with the nonresonant background (thermal?) relaxation, it means that from 2 to 0.5 K this relaxation is slowing down by more than an order of magnitude.

Extrapolations of the high-temperature susceptibility[10,13] suggested that ferromagnetic coupling between the clusters becomes important at temperatures approaching 50 mK. Our low-temperature data indicated no anomalies which we could attribute to such intercluster interactions.

To lowest order, the Hamiltonian for an $S=10$ system can be written as $\mathcal{H}_0=D_1S_z^2-\mu_B\mathbf{B}\cdot\overleftrightarrow{g}\cdot\mathbf{S}$. Here we assume axial symmetry, as is the case for the Mn_{12}-acetate crystal. We may restrict ourselves to $B_y=0$ without loss of generality, and then with $S_x=\frac{1}{2}(S^+ + S^-)$ and introducing the angle θ between the direction of the applied magnetic field and the easy axis (z), we can rewrite

$$\mathcal{H}_0=D_1S_z^2-g_{\|}\mu_B B\cos(\theta)S_z-\frac{1}{2}g_{\perp}\mu_B B\sin(\theta)(S^+ + S^-). \tag{1}$$

The eigenstates $|S,m\rangle$ are a convenient basis for the calculation of the matrix: recall that $S^{\pm}|S,m\rangle = \sqrt{(S\mp m)(S\pm m+1)}|S,m\pm 1\rangle$. D_1 describes the axial anisotropy energy, and is a negative number, so that the $m=\pm 10$ levels will be lowest in energy. The energy level diagram, obtained by direct diagonalization of $\mathcal{H}_0$ with $\mathbf{B}$ almost parallel to the c axis ($\theta=0.5°$), is shown in Fig. 4. As noted earlier also[2] for this simple Hamiltonian all level crossings occur at consecutive resonant magnetic fields B_N which are equally spaced: $B_N=N|D_1|/g\mu_B$.

One of the striking features of the Mn_{12} system is that below the blocking temperature (where the relaxation time starts to exceed the time of measurement) enhanced relaxation rates were found around these resonances[3,5] and it was therefore suggested that tunneling may be effective in reversing the magnetization. Above the blocking temperature the relaxation was found to be single exponential and thermally activated, $\tau=\tau_0\exp(K/k_BT)$. The effective energy barrier is

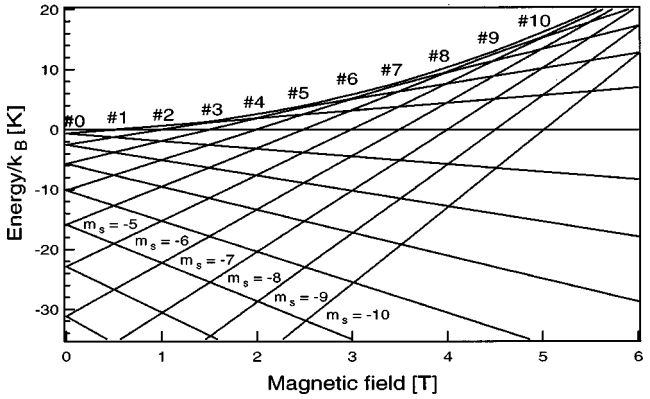

FIG. 4. Energy level diagram corresponding to the Hamiltonian $\mathcal{H}_0$ and calculated for a zero-field barrier of $64k_B$.

$|D_1|S^2$, and can be directly compared with the potential energy K from the thermal activation studies:[10] $D_1 \approx -0.64k_B$. EPR measurements show[8,9] that the axial anisotropy in the Hamiltonian is of the order $|D_1| = 0.5-0.6$ cm^{-1} with $g = 1.9$. This would correspond to an anisotropy barrier $100|D_1| = 72-86k_B$. The resonant fields observed in our measurement are shown in Fig. 5, as a function of index, and a linear fit to these data gives for the step size $\Delta\mu_0 H = 0.450 \pm 0.004$ T, in good agreement with other work.[3,5] With $g = 1.9$, the spacing between resonant steps observed in our experiment would lead to $57k_B$, significantly lower than the values inferred from EPR.[9] Using a sensitive EPR cavity perturbation technique we have probed the energy level diagram of the Mn_{12} acetate close to the top of the magnetization reversal barrier over the frequency range 35 to 115 GHz. The results of that study will be published elsewhere:[14] for the high-lying levels we find a g factor $g_{\|} \approx 2.05$, significantly higher than the published values. With $g = 2.05$ the barrier height inferred from the step ΔB comes quite close to $64k_B$. When discussing the Hamiltonian below, we will give some indications how the remaining differences may be reconciled.

RELAXATION OF THE MAGNETIZATION

It was suggested[3] that the relaxation time $\tau = 1/\Gamma$ associated with the reversal of magnetization would be simply related to the derivative of the magnetization curve times the ramping rate: $\Gamma = -(dM/dH)(dH/dt)$. Figure 6 shows a number of hysteresis curves, recorded at 1.40 K, for magnetic field ramping rates spanning the range from 0.0008 to 0.085 T/s, and the inset gives the derivative dM/dB. As the rate is lowered, the low field step ($N = 5$ in this case) starts to develop more clearly. This also implies that the magnetization will be completely reversed at a lower magnetic field than that at higher ramping rates. It can also be seen in the curves at this high temperature, that the slope between the resonant steps is not negligible. Thus our data suggest that the abovementioned simple relation for Γ does not hold, because (a) the resonant steps all seem to have similar width of 0.2 ± 0.1 T, independent of temperature and step index, and the dwell time observed is not strictly proportional to the ramping rate dH/dt; (b) what is observed is a step in the magnetization occurring over the time interval that the system is on resonance.

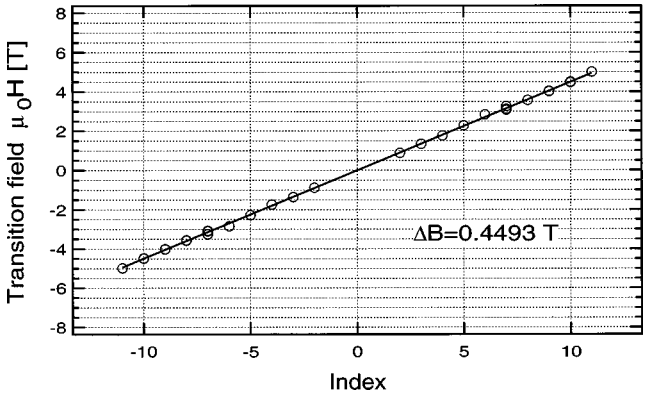

FIG. 5. Magnetic fields at which the magnetization was found to change rapidly, as a function of step index N. The slope of the linear fit gives the step separation.

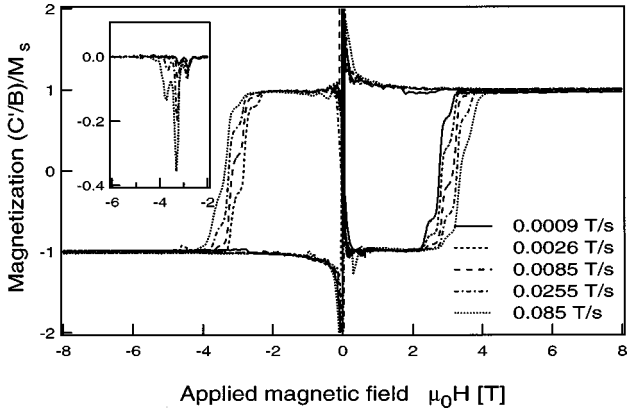

FIG. 6. Steps in the magnetization (normalized to the saturation magnetization M_s) for a Mn_{12}-acetate single crystal, measured at different ramping rates of the applied magnetic field. The derivatives dM/dB for four different rates, shown in the inset, illustrate that the derivative is not simply proportional to the ramping rate.

As has been realized earlier by others[3] the resonance may be shifted by the internal field, and for complete saturation of the magnetic moment, the contribution of the magnetization to the total field is as much as ± 0.06 T, not much lower than the widths of the resonances observed. When a significant part of the magnetization is reversed on a step, a significant shift in magnetic field B will have taken place towards higher fields, so that the dwell time on a step will be determined both by the ramping rate and the magnitude of the step in the magnetization. The step sizes, measured at different ramping rates and two different temperatures, are compiled in Fig. 7. Only for the lowest two indices ($N = 5$ for 1.4 K, and $N = 7$ for 0.5 K), an approximately linear increase with dwell time is observed, a prerequisite for the expression for Γ to be valid. In general, saturation is soon observed at the larger steps. The actual relaxation rates may then be found by shifting a straight line corresponding to a linear function of the dwell time, so that the observed magnitudes of the steps asymptotically approach the line. The dashed lines in the figure indicate the relaxation rates, and they shift to higher rates with increasing magnetic field ($=$index N) and for the same N to lower rates with decreasing temperature, as intuitively expected. We thus find $0.0012M_s/\mathrm{s}$ (τ

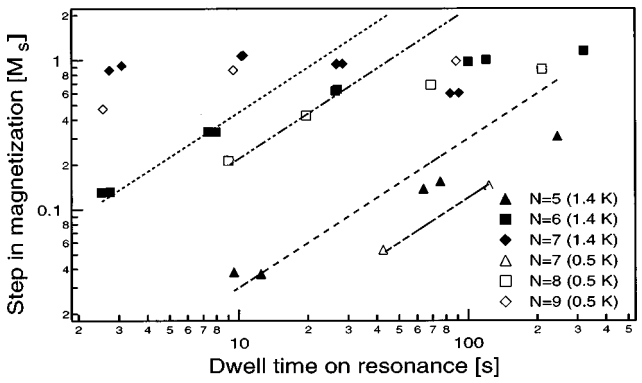

FIG. 7. Step size observed at resonance for varying ramping rates of the magnetic field, here plotted as a function of dwell time on resonance, shows that saturation easily occurs. The initial slopes (at high ramping rates and indicated by the dashed lines) range from $0.001M_s/\mathrm{s}$ for $N=7$ at 0.5 K to $0.05M_s/\mathrm{s}$ for $N=6$ at 1.4 K.

$=800$ s) for $N=7$ at 0.5 K and more than an order of magnitude increase in rate per unit of index. A rough estimate then gives that in lowering the temperature from 1.4 to 0.5 K the relaxation rate at a given step is decreasing with a factor 400–500. This is again in sharp contrast with the leveling off of the relaxation rates reported for other subkelvin temperature experiments.[6]

In another series of experiments, the crystal was fully magnetized by applying a high enough magnetic field (around 9 T in our case), and then the field was reversed and ramped up to a value corresponding to a step in the magnetization curve. Figure 8(a) shows the relaxation of the magnetization observed at different values of the magnetic field, corresponding to $N=7$, 8, and 9. Note that for indices 8 and 9 the relaxation on reaching the step is so rapid that a part of the change has occurred before t_0, especially so for the higher temperatures. During the first 250–500 s there is an exponential decay characterized by $\tau\approx 300$ s for $N=7$, and faster ($\tau\approx 100$ s) for $N=9$, with a total variation of magnetization of at most $0.2M_s$. For longer times the relaxation becomes logarithmic. These results clearly imply that the relaxation process is not governed by thermal excitation over a single barrier. Instead, a broad probability distribution of anisotropy barriers would account for such a time dependence.[15,16] The general idea is that starting at the lowest barrier, the system will automatically reach a barrier at which the lifetime of the metastable states becomes longer than the observation time in the experiment. A temperature-independent viscosity $S=\partial M/\partial(\ln t)$ may then be evidence for quantum tunneling.[16] The relaxation time observed in this experiment is *not* the relaxation time *at* the step, but rather *between* the resonances. When at constant field, the system will move out of resonance because of the change in internal field B as the magnetization is partially reversed.

This is very clearly shown in Fig. 8(b) which illustrates an experiment where the magnetic field was increased to resonant condition. A small modulation (with peak to peak variations ranging from 0.02 to 0.25 T in the experiment) was superimposed on the constant magnetic field, and the system was seen to go through the resonance as in the ramped field experiments, but it reentered resonance when the field was again in the appropriate range. There is a strong enhancement of the relaxation when the dwell time at resonance is increased by modulation compared to the case when the field is held constant. The data of Fig. 8(b) were obtained at 0.5 K, using fast-ramping resistive magnets with ramping rates used up to two orders of magnitude faster than that of the superconducting magnet. For the 60, 400, and 750 mK data in Fig. 8(a) the ramping rate of the superconducting magnet was 0.01 T/s at most: only at very low temperatures, e.g., 60 mK, there is a significant population of metastable excited states left after the fast relaxation while the system is in resonance, and this small remaining nonequilibrium population contributes to the slow relaxation. At higher temperatures, thermal excitation is so fast that the nonequilibrium population becomes depleted before it can contribute to a significant long time logarithmic decay. This shows three facts: (a) at low temperature and off resonance the deep-lying metastable states (e.g., the $m=-10$ level) cannot significantly contribute to spin reversal; (b) the observation of steps and relaxation is strongly dependent on history; and (c) the magnetic viscosities at 60 and 500 mK are not very much different at $S\approx 0.05$.

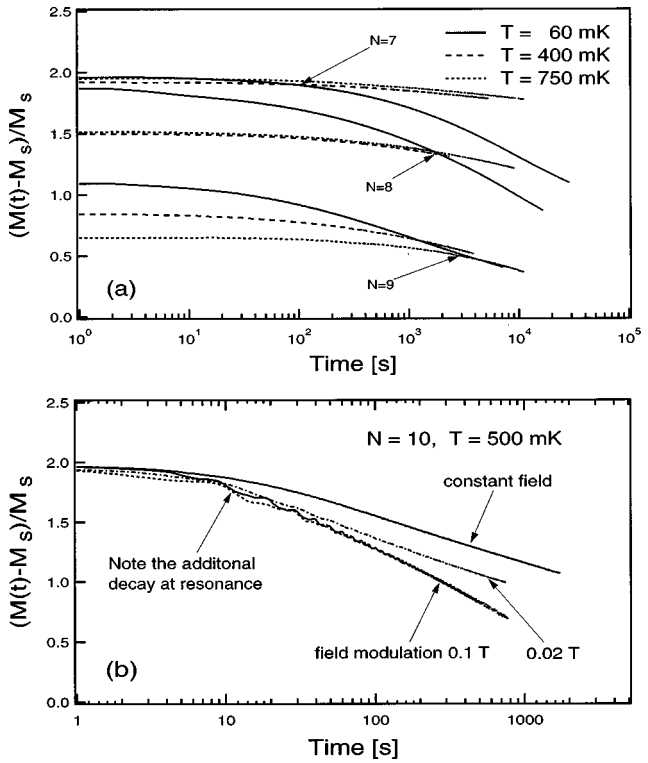

FIG. 8. Slow decay of the magnetization: Although exponential at short times, for longer times the decay is logarithmic. (a) With the magnetic field held constant at the resonant field, at 60, 400, and 750 mK. (b) at the step $N=10$ and at 0.5 K. The lower curves show a clear enhancement of the slow magnetization reversal when a small modulation (of 0.10 or 0.05 Hz) is superimposed on the static field leading to reentry into resonance at regular intervals.

MECHANISMS FOR TUNNELING

Several authors have discussed mechanisms for tunneling across the anisotropy barrier and the current status in the literature has been recently reviewed by Hernandez and co-workers.[3] These authors surmise that the tunneling rate is

only appreciable from levels near the top of the anisotropy barrier, so that some mechanism is required to populate the excited levels. On the other hand, in-plane anisotropy or a perpendicular component of the magnetic field may bring about reversal of magnetization: a perpendicular field leads to precession of the magnetic moment and so the magnetic moment has a chance of being reversed. Theoretically, such processes have recently been successfully treated with instanton techniques,[17] and related studies of magnetization reversal in ensembles of superparamagnetic particles have laid much of the groundwork.[18]

An intriguing question is whether the Mn_{12} clusters will reverse magnetization collectively with a number of their neighbors. Our magnetization data down to below 60 mK showed no evidence for intercluster coupling, and it is therefore reasonable to assume that each individual cluster can freely reverse its magnetization. Recently it was pointed out[19] that for this particular system (where, at the step, all levels of different m in the anisotropy well line up each with a partner level in the other well across the barrier) and at resonance, excited states can exchange spin with a neighboring cluster effectively through the weak dipolar coupling, without the need to exchange energy with the bath. Although this process does not lead to magnetization reversal directly it may help to bring the spin to levels where it can be reversed through tunneling or thermal excitation.

Mechanisms for reversal of magnetization considered so far include phonon-assisted tunneling and generalized Orbach processes,[20] level mixing and the resulting tunneling,[21] and dipole-dipole coupling with other clusters.[19] The hyperfine coupling with the nuclear spin system is also significant with an expected broadening of the levels of $\sqrt{12}\times 400$ MHz.

In the following we will discuss two terms in the Hamiltonian that may lead to tunneling. (1) A perpendicular magnetic field $B_x = B\ \sin(\theta)$ such as resulting from an accidental misorientation (for $\theta = 0.5°$ $B_x > 0.04$ T at $B = 5$ T) and (2) higher-order anisotropy.

In the calculations underlying Fig. 4, the term proportional to B_x was deliberately taken into account for a misorientation of 0.5°. It is clear that significant mixing causes anticrossing of the levels $m = -1$ and $m = 0$ around $N = 1$, $m = -2$ and $m = -1$ around $N = 3$, etc., because they become degenerate just at the top of the barrier. At the even indices much weaker mixing will occur, between levels at an energy D_1 below the top, e.g., between $m = -6$ and $m = -4$ at $N = 10$. Our calculations show that the gap opening between the $m = -5$ and $m = -4$ levels at $N = 9$ equals $0.46 k_B \propto 9.5\times 10^9\ s^{-1}$, while the gap between $m = -6$ and $m = -4$ at $N = 10$ is $0.21 k_B \propto 4.3\times 10^9\ s^{-1}$. The level mixing and resulting tunneling rate was calculated using higher-order perturbation theory,[21] and such calculations are very appropriate when the mixing is weak. The level structure near the top of the well is quite different for the even and odd magnetization steps, as illustrated in Fig. 9. We recalculated the tunneling rate following Garanin's approach taking into account the details of the level structure at the top of the well and explicitly considering the gap and mixing between the two degenerate levels. The results are shown in Table I. The results suggest weak oscillations between even and odd transitions; these, however, have not been observed so far.

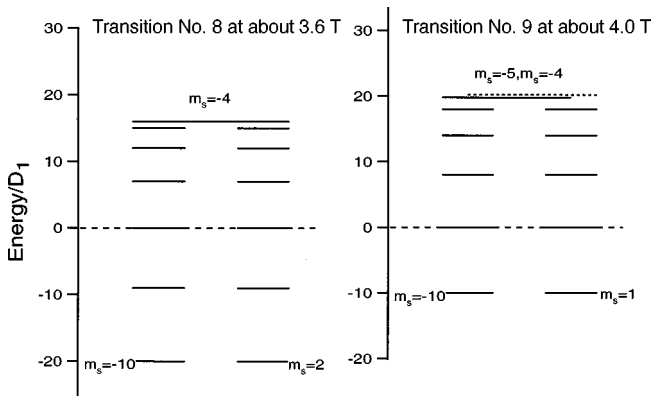

FIG. 9. Energy level diagram near the top of the anisotropy barrier for $\mathcal{H}_0$. For the even steps the interlevel spacings grow as $D_1, 3D_1, 5D_1, \ldots$, and for the odd steps as $\approx 2D_1, 4D_1, 6D_1, \ldots$. Note that for odd steps two levels become degenerate at the top of the barrier, and the transverse magnetic field will lead to significant mixing of these levels.

In thermal equilibrium at 1 K and for a field corresponding to step $N = 8$, only about 1 in 10^9 of the clusters will be in the excited state $m = -6$ (i.e., about 6×10^6 spins in our samples), and about one order of magnitude more for each additional step. On the other hand, the coupling with a state across the top of the barrier is strong enough to instantaneously depopulate this level at fields above 4 T. The reason for this is easily seen in Fig. 10 where the energies of the levels for different m are plotted for magnetic fields corresponding to step index 8, 9, and 10. The barrier for excitation from the $m = -10$ level is significantly lower than the zero-field barrier of $64 k_B$ (indicated by the dashed horizontal line), and the $m = -6$ level is very close to the top of the anisotropy barrier for these steps. Nevertheless, at much lower temperatures, one would expect that the exponential decrease of the population in the excited level would prevent further magnetization reversal through that level.

There may be reasons why the excited levels become more effectively populated: It is also apparent in Fig. 10 that the energy of the $m = +10$ level is deepening and that there will be an increasing release of potential energy when a state near the top of the barrier decays to the stable $m = 10$ state: in fact up to $130 k_B$ per cluster, as much as 10 μJ for a 20 μg crystal when the reversal takes place at 4 T. If the heat is not transferred to the thermal sink sufficiently fast the repopulation of the excited levels may correspond to a much higher temperature than the temperature of the bath. Jumps of magnetization reversal taking place within milliseconds have been observed[13] and these ''avalanches'' do indeed show little dependence on ramping rate and bath temperature. In their experiment, Paulsen and coworkers had placed the superconducting quantum interference device and sample onto a heat exchanger outside the mixing chamber in the vacuum, in our experiment the cantilever and crystal were immersed in the liquid in the mixing chamber (or in the ^{3}He), providing much more efficient heat transfer out of the crystal. We are presently investigating the rates at which heat is produced upon reversal of the magnetization in an attempt to estimate the temperature internal to the crystal. The fact that the slope *between* the steps varies over the range of temperatures and tends to zero seems to indicate however, that in our

TABLE I. Tunneling rates between some of the levels near the top of the anisotropy barrier as a result of a weak perpendicular magnetic field, such as caused by 0.5° misorientation. The initial and final states are labeled by m_i and m_f, their energy $E_m - E_t$ is measured with respect to the top of the barrier, and the rate is given by the gap opening between the degenerate levels $\Delta E/h$.

m_i	m_f	$E_m - E_{-10}$	n_{thermal}	$E_m - E_t$	Rate [1/s]
		(Step at $N=8$, $B \approx 3.59$ T)			
-7	-1	$27\lvert D_1\rvert$	3×10^{-8}	$-9\lvert D_1\rvert$	2.5×10^{3}
-6	-2	$32\lvert D_1\rvert$	1×10^{-9}	$-4\lvert D_1\rvert$	9.4×10^{6}
-5	-3	$35\lvert D_1\rvert$	2×10^{-10}	$-\lvert D_1\rvert$	3.1×10^{9}
		(Step at $N=9$, $B \approx 4.04$ T)			
-7	-2	$24\lvert D_1\rvert$	2×10^{-7}	$\approx -6\lvert D_1\rvert$	1.8×10^{6}
-6	-3	$28\lvert D_1\rvert$	2×10^{-8}	$\approx -2\lvert D_1\rvert$	0.73×10^{9}
		(Step at $N=10$, $B \approx 4.49$ T)			
-8	-2	$16\lvert D_1\rvert$	4×10^{-5}	$-9\lvert D_1\rvert$	6.6×10^{3}
-7	-3	$21\lvert D_1\rvert$	1×10^{-6}	$-4\lvert D_1\rvert$	19×10^{6}
-6	-4	$24\lvert D_1\rvert$	2×10^{-7}	$-\lvert D_1\rvert$	4.3×10^{9}

experiments the heat is effectively removed by the time the field has changed so much that the system is out of resonance. Typical values of the resonance width are 0.1–0.2 T, remarkably close to $\Delta B = 2\mu_0 M_s$.

Another mechanism that can promote magnetization to higher levels is the fourth-order term in the Hamiltonian. The tetragonal crystal symmetry forbids terms of the form $D_{1\perp}S_x^2$, but the fourth-order terms $\mathcal{H}_4 = D_{4\perp}(S_x^4 + S_y^4) + D_{4\parallel}S_z^4$ would be allowed,[22] and this term was also discussed in some detail in the context of phonon-assisted tunneling.[20] If we include the term $\mathcal{H}_4$ into the Hamiltonian of Eq. (1), we obtain

$$\mathcal{H} = +D_1 S_z^2 + D_{4\parallel}S_z^4 - g_\parallel \mu_B B\cos(\theta)S_z - \frac{1}{2}g_\perp \mu_B B \sin(\theta)(S^+ + S^-) + D_{4\perp}(S_x^4 + S_y^4). \quad (2)$$

We can rewrite S_x and S_y in terms of the raising and lowering operators S^+ and S^-:

$$(S_x^4 + S_y^4) = \frac{1}{8}(S^{+4} + S^{-4}) + \frac{3}{4}S_z^4 - \frac{1}{4}\{6S(S+1) - 5\}S_z^2 + \frac{1}{4}\{2S^2(S+1)^2 + (S-1)S(S+1)(S+2)\}. \quad (3)$$

The first term provides off-diagonal terms in the Hamiltonian coupling such levels as $m = -2$ with $m = +2$ or $m = -10$ with $m = -6$, the second and third terms contribute to the diagonal terms and will influence the spacing between the levels with different $|m|$ and the effective barrier height, and the fourth term in this expression just adds a constant level to the energy and can be neglected. Substitution of the results of Eq. (3) into the Hamiltonian of Eq. (2) leads to an expression that can be easily evaluated:

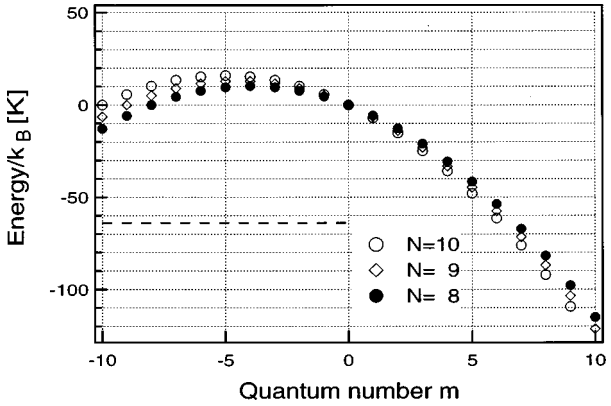

FIG. 10. Position of the energy levels at three different values of the magnetic field, corresponding to resonances $N=8$, 9, and 10, respectively. The dashed line is the energy of the $m = \pm 10$ levels at zero field, corresponding to the zero-field barrier height. The barrier for magnetization reversal is significantly reduced with these magnetic fields while the energy gained when a state near the top of the barrier decays to the stable $m = 10$ state is growing.

$$\mathcal{H} = \left\{D_1 - \frac{1}{4}D_{4\perp}(6S(S+1) - 5)\right\}S_z^2 + D_{4\parallel}S_z^4 + \frac{3}{4}D_{4\perp}S_z^4 - g_\parallel \mu_B B\cos(\theta)S_z - \frac{1}{2}g_\perp \mu_B B \sin(\theta)(S^+ + S^-) + \frac{1}{8}D_{4\perp}(S^{+4} + S^{-4}). \quad (4)$$

In the following we will assume that the anisotropy in the g factor and fourth-order anisotropy will be small: $g_\parallel, g_\perp \approx g$ and $D_{4\parallel}, D_{4\perp} \approx D_4$. We will then try to determine the magnitude of D_4 required to have a significant impact, and compare with the experimental data. The first observation is that the effective barrier height is now changed from $100|D_1|$ to $|100D_1 - 8875D_{4\perp} + 10{,}000D_{4\parallel}|$. If we define D_0 as one hundredth of the total height of the anisotropy barrier, we obtain for the energies at $B=0$:

$$E(m, B=0) = -D_0 m^2 - 100(0.75D_{4\perp} + D_{4\parallel})m^2 + (0.75D_{4\perp} + D_{4\parallel})m^4 \approx -(D_0 + 175D_4)m^2 + 1.75D_4 m^4 \quad (5)$$

For negative values of D_4 the levels of larger $|m|$ will be pulled increasingly strongly towards the bottom of the well, and therefore the energy levels appear to be compressed towards the top of the anisotropy barrier compared to the case of the Hamiltonian of Eq. (1).

The effect of a fourth-order anisotropy term with negative prefactor is twofold: (1) compression of the energy levels towards the top of the barrier will make it more probable that spins in an excited state will be moved up to the top of the barrier by thermal processes or across the barrier through the increased tunneling rates and (2) it reduces the spacing between the resonance fields for the excited levels possibly reducing the observed discrepancy with the associated barrier height. As the shifts are not any longer strictly proportional to m^2, the steps will not be equally spaced in this case. It should be noted that just this fact that all levels in the well

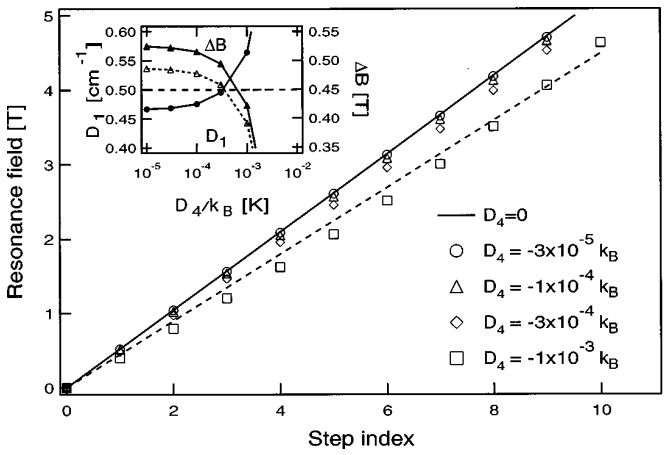

FIG. 11. Resonance fields as a function of step index N calculated for varying strengths of the fourth-order anisotropy D_4. The dashed line represents the measured steps. Note that with increasing D_4 the stepsize is effectively reduced. The inset shows that the apparent $D_1=\Delta_0/19$ and the apparent step size ΔB (solid line calculated with $g=1.90$, dashed line with $g=2.05$) tend to the experimentally determined values for $D_4\approx-5\times10^{-4}k_B$.

would come into resonance with a level across the barrier at the same time was attractive and has enticed earlier workers to suggest quantum tunneling as the possible channel for reversal of magnetization. A direct consequence is also that the zero-field splitting between the $m=-10$ and $m=-9$ levels, for which EPR would be sensitive,[9] will be relatively bigger (i.e., $>19/100\times$barrier height). The presence of the fourth-order anisotropy can possibly explain why systematically high values were derived from the zero-field offset measured in EPR.

We have tried to estimate the impact of D_4 by calculating the resonance fields at which level crossings occur, only taking the diagonal terms of Hamiltonian Eq. (4). In all these calculations we adjusted D_1 to obtain a constant effective barrier height $100D_0$. The results are shown in Fig. 11, together with the resonance fields observed in the experiment. The inset shows both the apparent stepsize and the apparent D_1 [taken as the fraction ($\frac{1}{19}$) of the zero-field splitting]. The position of the level crossings depends critically on g: the solid curve corresponds to the data in Fig. 11 and was obtained with $g=1.9$,[9] the dashed curve with the higher g value of 2.05 found in our work.[14] The two curves tend to the experimentally determined values around $D_4=3\times10^{-4}k_B$, strongly suggesting that fourth-order anisotropy is important, and giving circumstantial support for the value $g_\parallel=2.05$. The linearity observed in the resonance fields as a function of magnetic field puts a limit to D_4: for values exceeding $3\times10^{-4}k_B$ deviations from linearity are larger than the widths of the resonances.

It is illustrative to compare the effect of the D_4 contribution on the zero-field offsets with the original EPR measurements at very high frequencies[8,9] and our own EPR studies at much lower frequencies.[14] For the Hamiltonian $\mathcal{H}_0$ of Eq. (1), the energy levels are given by D_1m^2, and hence the separation between the levels m and $m-1$ for which EPR with the field along the easy axis will be sensitive is given by $(2m-1)D_1$, linearly increasing with m. In Fig. 12 the dashed line represents the zero-field offsets that would be

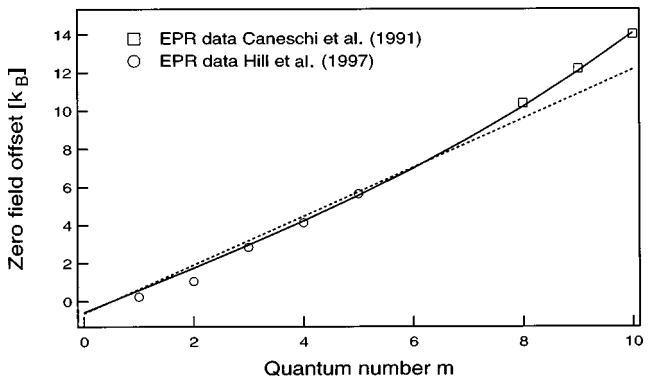

FIG. 12. Zero-field offsets measured by Caneschi and coworkers for frequencies between 245 and 525 GHz, and preliminary data from this study for the frequency range below 115 GHz, and for magnetic field directed parallel to the easy axis. The dashed line is the prediction using $\mathcal{H}_0$, while the solid line represents a Hamiltonian including fourth-order anisotropy.

predicted with $\mathcal{H}_0$ and the solid line those predicted by Hamiltonian Eq. (4), with $D_4=-5\times10^{-4}k_B$. A fit with this value of D_4 and assuming a somewhat higher barrier height of $67k_B$ is in remarkably good agreement with the high frequency EPR data[8,9] and our preliminary data at lower frequencies (and hence higher-lying levels).

Mixing of the ground energy level $m=-10$ with the excited level $m=-6$ can in principle be a very effective way to promote spins to the excited levels, from which they can easily tunnel through or be excited over the top of the barrier. Around $B=4$ T and for $D_4=-5\times10^{-4}k_B$ the off-diagonal elements lead to 0.5% admixture of $|-6\rangle$ into $|-10\rangle$, the admixture decreases somewhat with decreasing field to about 0.3% at 2 T. For comparison, at 1 K and 4 T, the thermal excitation from the metastable level $m=-10$ to $m=-6$ would be only 10^{-9}, and four orders of magnitude smaller at 2 T, while the time to reestablish thermal equilibrium is probably very long. The mixing of the levels, due to the fourth-order term is therefore very effective in the enhancement of tunneling from higher levels in the well. We contend therefore that it is primarily the fourth-order anisotropy, in combination with tunneling and possibly dipole-dipole exchange and the subsequent rapid exothermal descent to the $m=+10$ level, which drives the reversal of magnetization in the Mn_{12} clusters. It is therefore no surprise that spin reversal becomes essentially instantaneous as soon as the $m=-6$ level comes close to the top of the barrier, i.e., at step $N=10$. At $N=8$, the fourth-order coupling between the degenerate levels $m=-6$ and $m=-2$, leads for $D_4=-1\times10^{-4}k_B$ to a splitting of as much as $0.22k_B$ (4.5×10^9 s^{-1}), which is much stronger than the B_x-driven tunneling across the $4D_1$ high barrier which we calculated in Table I. One would therefore expect a dramatically increased efficiency of the relaxation process. When redistribution through dipole-dipole coupling is sufficiently effective, one can speculate that the tunneling at all even steps will be primarily through the fourth-order anisotropy term.

CONCLUSIONS

We have studied the reversal of magnetization in Mn_{12} acetate using a very sensitive cantilever magnetometer. We

have observed clearly resolved steps in the magnetization, believed to be related to quantum tunneling of magnetization, for temperatures down to below 60 mK. Contrary to expectations, we have observed steps up to index $N=11$ only. The reversal of magnetization is very fast when the field is brought to any of the resonances, and the step seems to be limited in size because the change in internal field eventually breaks the alignment of the energy levels on two sides of the anisotropy barrier between which the tunneling occurs. Upon magnetization reversal a significant amount of energy is released, and we contend that it is primarily reabsorption of phonons which drives the repopulation of tunneling excited states. Analysis of ramping-rate-dependent data at 1.4 and 0.5 K, revealed a clear temperature dependence with a 500-fold decrease of decay rates at resonance between these two temperatures, in marked contrast to observations in the literature of saturation of the relaxation rates below 1 K. After detuning from the resonance, we find that the magnetization reversal is very slow and is logarithmic rather than single exponential. This indicates that, in this phase, a number of processes must take part in the decay process and it is plausible that the small excess population left in excited levels, will decay in part down to the metastable $m=-10$ state and in part, after phonon-assisted tunneling or thermal excitation over the top of the barrier, towards the stable $m=+10$ level.

ACKNOWLEDGMENTS

Part of this work was performed at the National High Magnetic Field Laboratory, which is supported by NSF Cooperative Agreement No. DMR-95-27035 and by the State of Florida. This work was also supported by the National Science Foundation under Grant No. DMR 95-10427. One of us (J.A.A.J.P.) acknowledges support and hospitality of NHMFL during his stay in Tallahassee. We are grateful to J. Qualls, T. Stalcup, J. Cothern, and S. Han who assisted with some of the measurements, and to E. Palme and C. Wolter for access to the millikelvin facilities and cantilever magnetometer.

Note added. Recently, A. L. Barra and co-workers [Phys. Rev. B **56**, 8192 (1997)] also reported evidence for a fourth-order term in the crystal-field anisotropy. They have used a different notation, in terms of coefficients B_4^4 and B_0^4. The connection between our Hamiltonian of Eq. (4) and their expressions is the following: $B_4^4=\frac{1}{4}D_{4\perp}\approx\frac{1}{4}D_4$ and $B_4^0=\frac{1}{20}\{\frac{3}{7}D_{4\perp}+\frac{4}{7}D_{4\|}\}\approx\frac{1}{20}D_4$.

[1] T. Lis, Acta Crystallogr., Sect. B: Struct. Crystallogr. Cryst. Chem. **36**, 2042 (1980).
[2] Jonathan R. Friedman, M. P. Sarachik, J. Tejada, and R. Ziolo, Phys. Rev. Lett. **76**, 3830 (1996).
[3] J. M. Hernandez, X. X. Zhang, F. Luis, J. Tejada, Jonathan R. Friedman, M. P. Sarachik, and R. Ziolo, Phys. Rev. B **55**, 5858 (1997).
[4] F. Luis, J. Bartolomé, J. F. Fernández, J. Tejada, J. M. Hernández, X. X. Zhang, and R. Ziolo, Phys. Rev. B **55**, 11 448 (1997).
[5] L. Thomas, F. Lionti, R. Ballou, D. Gatteschi, R. Sessoli, and B. Barbara, Nature (London) **383**, 145 (1996).
[6] C. Paulsen, J.-G. Park, B. Barbara, R. Sessoli, and A. Caneschi, J. Magn. Magn. Mater. **140–144**, 379 (1995).
[7] C. Sangregorio, T. Ohm, C. Paulsen, R. Sessoli, and D. Gatteschi, Phys. Rev. Lett. **78**, 4645 (1997).
[8] R. Sessoli, H.-L. Tsai, A. R. Scake, S. Wang, J. B. Vincent, K. Folting, D. Gatteschi, G. Christou, and D. N. Hendrickson, J. Am. Chem. Soc. **115**, 1804 (1993).
[9] A. Caneschi, D. Gatteschi, R. Sessoli, A. L. Barra, L.-C. Brunel, and M. Guillot, J. Am. Chem. Soc. **113**, 5873 (1991).
[10] M. A. Novak, R. Sessoli, A. Caneschi, and D. Gatteschi, J. Magn. Magn. Mater. **146**, 211 (1995).
[11] R. Sessoli, D. Gatteschi, A. Caneschi, and M. A. Novak, Nature (London) **365**, 141 (1993).
[12] M. Chaparala, O. H. Chung, and M. J. Naughton, in *Superconductivity and its Applications*, AIP Conf. Proc. No. **273**, edited by H. S. Kwok, D. T. Shaw and M. J. Naughton (American Institute of Physics, New York, 1992), p. 407.
[13] C. Paulsen, J.-G. Park, B. Barbara, R. Sessoli, and A. Caneschi, J. Magn. Magn. Mater. **140-144**, 1891 (1995).
[14] S. Hill, J. A. A. J. Perenboom, N. S. Dalal, T. Hathaway, T. Stalcup, and J. S. Brooks, Phys. Rev. Lett. **80**, 2453 (1998).
[15] J. Tejada and X. Zhang, in *Quantum Tunneling of Magnetization—QTM'94*, Vol. 301 of *NATO Advanced Studies Institute, Series E: Applied Sciences*, edited by L. Gunther and B. Barbara (Kluwer, Dordrecht, 1995), p. 121.
[16] L. Gunther, in *Quantum Tunneling of Magnetization—QTM'94* (Ref. 15), p. 413.
[17] For a review of the state of the art see contributions in *Quantum Tunneling of Magnetization—QTM'94* (Ref. 15)
[18] B. Barbara, W. Wernsdorfer, L. C. Sampaio, J. G. Park, C. Paulsen, M. A. Novak, R. Ferré, D. Mailly, R. Sessoli, A. Caneschi, K. Hasselbach, A. Benoit, and L. Thomas, J. Magn. Magn. Mater. **140-144**, 1825 (1995).
[19] A. L. Burin, N. V. Prokof'ev, and P. C. E. Stamp, Phys. Rev. Lett. **76**, 3040 (1996).
[20] P. Politi, A. Rettori, F. Hartmann-Boutron, and J. Villain, Phys. Rev. Lett. **75**, 537 (1995).
[21] D. A. Garanin, J. Phys. A **24**, L61 (1991).
[22] J. Villain, F. Hartmann-Boutron, R. Sessoli, and A. Rettori, Europhys. Lett. **27**, 159 (1994).